Interterminal Distance and Flexibility of a Triantennary Glycopeptide As Measured by Resonance Energy Transfer†

Kevin G. Rice, Pengguang Wu, Ludwig Brand, and Yuan C. Lee*
Department of Biology, Johns Hopkins University, Baltimore, Maryland 21218
Received January 22, 1991; Revised Manuscript Received March 28, 1991

ABSTRACT: Three geometric isomers of a single triantennary glycopeptide, each containing two fluorophores attached to terminal positions in the molecule, were used to probe distance and flexibility of the oligosaccharide in solution. A dansyl group (energy acceptor) was attached to the C6 of Gal at either position 6′, 6, or 8, and a naphthyl-2-acetyl group (energy donor) was coupled to the N terminus of the Ala-Asn peptide.

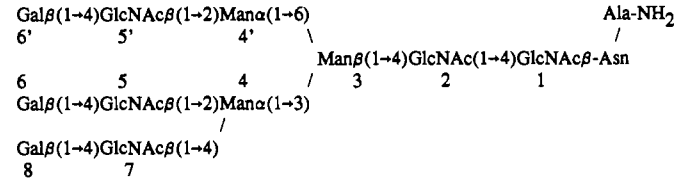

Resonance energy-transfer measurements revealed an average distance of approximately 22, 18, and 17 Å between the donor and the acceptor attached to either the 6, 8, or 6′ Gal residue, respectively. The lifetime of the donor's emission was nearly a single-exponential decay of 27 ns (96%), whereas the decay of the donor with proximally attached acceptor was fit by nonlinear least-squares analysis to a multiexponential for each glycopeptide probe. Fitting with a Lorentzian function revealed spatially distinct donor/acceptor distances presumably arising from glycopeptide branch flexibility. The results suggest that the acceptor located at Gal 8 is the most rigid relative to the donor with a single population of distances centered at 18.4 Å. In contrast, the acceptor attached to either Gal 6′ or 6 displayed two populations of different distances from the donor. The Gal 6 isomer contained a major population with average donor/acceptor separation distance of 21.7 Å and a minor population with average separation distance of 9.7 Å. Similarly, the Gal 6′ isomer showed a major population with donor/acceptor separation distance of 18.3 Å and a minor population with separation distance of 11.7 Å. These data support the earlier conclusions that the Manα(1→6)Man linkage found in the core pentasaccharide of all branched N-linked oligosaccharides is flexible. In addition, the data suggest that the branch containing Gal 6 is also flexible in the triantennary glycopeptide.

Complex N-linked oligosaccharides are found in many glycoproteins such as receptors, hormones, immunoglobulins, and enzymes and occur as the result of extensive posttranslational processing of "high mannose" type oligosaccharides (Kornfeld & Kornfeld, 1985). Although the function(s) of these oligosaccharides remains to be determined, a clustered arrangement of terminal Gal residues is necessary for tight binding to endogenous mammalian lectins, including the ASGP-R[1] of hepatocytes (Lee et al., 1983). A complex triantennary glycopeptide binds to the rat ASGP-R in a unique precise geometry (Rice & Lee, 1990), in accord with the possibility that each branch of the triantennary oligosaccharide is placed specifically in a unique conformation.

The solution conformations of a variety of N-linked oligosaccharides have been rigorously investigated with use of data derived from proton NMR and theoretical modeling to arrive at most probable conformations about each glycosidic linkage (Brisson et al., 1983a,b,c; Bock et al., 1982; Cummings et al., 1987; Cummings & Carver, 1987a,b; Homans et al., 1986, 1987a,b,c; Edge et al., 1990). Several groups have proposed that the Manα(1→6)Man linkage found in the core region of all N-linked oligosaccharides is the major site of flexibility in these oligosaccharides (Brisson et al., 1983b; Montreuil, 1984; Cummings et al., 1987c; Homans et al., 1986).

One limitation in using NMR data for deciphering solution conformations is that the measured NOE and coupling constant are the result of conformational averaging over the millisecond time scale providing only virtual data for the determination of conformation (Cummings et al., 1987a). Interpretation of the experimental data in light of calculated preferred conformations refines the results; however, simulations are limited by computational burden to minimize the energy of only a few selected bond angles in a single experiment, and most reports do not account for the influence of solvent on conformational stabilization.

Stryer has demonstrated the use of fluorescence energy transfer as a molecular ruler to measure distances in biopolymers ranging from 20 to 50 Å (Stryer & Haugland, 1967). Studies utilizing fluorescence energy transfer have previously been performed on proteins, oligonucleotides, and lipid biopolymers (Fairclough & Cantor, 1977; Stryer, 1978, and references therein) but not on the complex carbohydrates. This

† Supported by NIH Research Grant DK09970 (Y.C.L.), NIH Grant GM11632 (L.B.), and Postdoctoral Fellowship GM 13013-01 Bi-4 (K.G.R.).
* To whom all correspondence should be addressed.

[1] Abbreviations: ASGP-R, asialoglycoprotein receptor; NMR, nuclear magnetic resonance; NOE, nuclear Overhauser effect; RP-HPLC, reversed-phase high-performance liquid chromatography; ASOR, asialoorosomucoid; DCM, 4-(dicyanomethylene)-2-methyl-6-(*p*-(dimethylamino)styryl)-4*H*-pyran; R6G, rhodamine 6G; NATA, *N*-acetyltryptophanamide.

0006-2960/91/0430-6646$02.50/0

is due in part to the difficulty in selective attachment of fluorophores to oligosaccharides at known positions. Once prepared, steady-state measurements of donor quenching and acceptor sensitized emission can be used to calculate the average distance separating the donor from the acceptor by the Förster equation (Förster, 1948). When flexible polymers are used to space fluorophores, donor fluorescence lifetime decay curves may be fit by a nonlinear least-squares method to dissect components with different decay rates (Haas et al., 1975). The interpretation of these data, as distributions of donor and acceptor separated by different distances, has allowed extension of this technique to measure flexibility in biopolymers.

In an effort to seek alternative forms of data that can increase the understanding of the solution conformation of oligosaccharides, we propose the use of fluorescence energy transfer to measure both the interterminal distance and the flexibility of complex glycopeptides in solution. The difficulty of introducing a fluorescence donor and acceptor into known locations of the molecule may be solved by using oligosaccharides that allow attachment of fluorophores to the reducing end and terminal Gal residues after enzymatic oxidation. Alternatively, complex asialoglycopeptides allow introduction of the fluorescent groups into the C or N terminus of the peptide and may also be oxidized with galactose oxidase to introduce a second site for specific attachment of fluorophores.

Fluorescence energy-transfer studies on branched oligosaccharides differ from other similar studies on biopolymers. The oligosaccharides are devoid of interfering absorbance, can be purified to homogeneity after attachment of fluorophores without denaturation, and contain both rigid and semiflexible character in the same molecule. In addition these molecules serve as ligands for mammalian receptors; thereby, energy transfer might be useful to reveal the conformation of the receptor-bound ligand.

The data obtained from this approach complements NMR conformational studies of oligosaccharides in the following ways: interterminal distances in the molecule can be determined directly without summing bond angles around individual glycosidic linkages; fluorescence lifetime measurements are acquired on the nanosecond time scale, which results in the direct measurement of one or more population of donor/acceptor distances; and the measurements are performed on the microanalytical scale, allowing the use of energy transfer in conjunction with exoglycosidase reactions to detect changes in oligosaccharide structure after removal of terminal sugar residues. In the present study we have applied some of these aspects of energy transfer to study the solution conformation of the triantennary glycopeptide ligand of the ASGP-R.

Materials and Methods

Chromatography was performed on a Gilson gradient HPLC equipped with a Fiatron column oven (50 °C), an ISCO V4 UV/vis variable wavelength detector, and a Perkin-Elmer LS40 scanning fluorescence detector. Spherisorb HPLC columns were purchased from Phase Separation (Norwalk, CT).

Glycopeptide Preparation, Characterization, and Binding Activity. The detailed preparation of fluorescent glycopeptide probes utilized in this study (Figure 1) has been published elsewhere (Rice & Lee, 1990). A brief description of the synthesis of these probes is described below. A single triantennary glycopeptide from bovine fetuin was partially oxidized with galactose oxidase. The seven isomers resulting from partial reaction were resolved on RP-HPLC after formation of (2,4-dinitrophenyl)hydrazones. The individual purified glycopeptide hydrazones were reverted to the corresponding triantennary oxoglycopeptides. The proton NMR spectra of each individual mono-, di-, and trioxoglycopeptide allowed identification of the location of the oxidized Gal residue(s). Dansylethylenediamine was coupled to the C6 aldehyde of Gal by reductive amination to prepare glycopeptides designated GP-6-Dan, GP-6′-Dan, and GP-8-Dan, where the underlined number indicates to which Gal residue the dansyl group is attached (Figure 1). Naphthyl-2-acetic acid was then attached to the N terminus of alanine via its succinimidyl ester to prepare glycopeptides termed GP-6-DanNap, GP-6′-DanNap, GP-8-DanNap, and GP-Nap. All of the isomers were purified to homogeneity on RP-HPLC and characterized by quantitative monosaccharide and amino acid analysis and scanning UV/vis and fluorescence spectroscopy.

RP-HPLC was performed on an octyl column (0.47 × 25 cm) eluted with 10 mM ammonium acetate, pH 5.0 (A) and a gradient of acetonitrile (B) (0 min, 10%; 7 min, 10%; 15 min, 18%; 40 min, 27%). Fluorescence detection utilized 50-pmol sample injections, and UV_{220nm} detection required 200 pmol of sample.

Inhibition assays were used to assess the binding affinity of the fluorescent glycopeptides as described previously using ^{125}I-ASOR as the primary ligand for binding to the ASGP-R on isolated rat hepatocytes (Rice et al. 1990).

Spectroscopic Measurements. Absorption spectroscopy was performed on a Perkin-Elmer LS spectrophotometer, and steady-state fluorescence spectra were acquired on an SLM 8000 photon counting spectrophotofluorometer. The absorbance of all samples was below 0.1 at the wavelength of excitation. Correction of naphthyl-2-acetyl emission spectra was performed with reference to a corrected spectra for NATA.

Time-resolved fluorescence decays of the naphthyl-2-acetyl derivatives of triantennary glycopeptides with and without dansyl were measured with use of a single photon counting apparatus as described earlier (Badea & Brand, 1979) with a picosecond synchronously pumped mode-locked dye laser to excite naphthyl-2-acetyl at 290 nm using R6G dye and to excite dansyl at 340 nm using DCM dye. The emission was detected at 350 nm for naphthyl-2-acetyl and at 520 nm for dansyl. Equal time collection on sample and buffer was employed to correct for background, and a Ludox solution was used to collect the instrument response. Corrections for the color effect of the photomultiplier tube were obtained with use of monoexponential standards (melatonin at 350 nm, which exhibits a single-exponential decay with a lifetime close to 5.5 ns, and 9-cyanoanthracene, which has a single lifetime of 12 ns in ethanol (Badea & Brand, 1979)). Triplicate data were collected for each sample at room temperature (20 °C).

Data Analysis

(A) Calculation of R_0. The Förster distance of 50% transfer efficiency (R_0) for naphthyl-2-acetyl and dansyl groups was calculated on the basis of (Förster 1948)

$$R_0^6 = 8.78 \times 10^{-5} k^2 \phi J n^{-4} \quad (1)$$

The orientation factor (k^2) was considered to be two-thirds on the assumption that the donor and acceptor pair can adopt random conformations (Englert & Leclerc, 1978; Haas et al., 1978). The quantum yield (Φ) of naphthyl-2-acetyl in GP-Nap dissolved in 5 mM phosphate, pH 7.0, was 0.095, using tryptophan ($\Phi = 0.14$) as a reference in water at pH 7.2, 25 °C (Eaton, 1988).

The fluorescence spectral overlap of donor emission with acceptor excitation (Figure 2A) allowed determination of the overlap integral using eq 2, where $F^{D\lambda}$ is the corrected emission

$$J = \frac{\int_0^\infty F^{D\lambda}\epsilon^{A\lambda}\lambda^4\, d\lambda}{\int_0^\infty F^{D\lambda}\, d\lambda} \quad (2)$$

spectra of the donor (GP-Nap) and $\epsilon^{A\lambda}$ is the molar absorptivity of the acceptor (GP-6-Dan) at each wavelength, which was 5.6×10^3 M^{-1} at 334 nm. The overlap integral (J) of the donor with acceptor was determined to be 5.61×10^{13} cm^{-1} M^{-1} nm^4.

The refractive index of the dilute glycopeptide samples (2×10^{-6} M) in 5 mM sodium phosphate, pH 7.0, was considered to be that of water ($n = 1.4$); therefore, the resulting R_0 calculated was 20.8 Å and the average distance $\bar{r}$ separating the donor and acceptor could be calculated with use of eq 3 after determination of efficiency (E).

$$\bar{r} = R_0\left(\frac{1 - E}{E}\right)^{1/6} \quad (3)$$

(*B*) *Steady-State Energy Transfer Measurement.* The efficiency of energy transfer (E) determined by donor quenching was calculated by

$$E = 1 - \left(\frac{F^{DA}}{F^D}\right) \quad (4)$$

where F^D is the integrated fluorescence intensity of donor alone (GP-Nap) and F^{DA} is the integrated intensity of donor in the glycopeptides containing a donor and acceptor. Alternatively, the efficiency was determined by sensitized emission of the acceptor by

$$E = \left(\frac{F^{DA_{280}}}{F^{DA_{334}}} - \frac{F^{D_{280}}}{F^{D_{334}}}\right)\left(\frac{\epsilon^{A_{334}}}{\epsilon^{D_{280}}}\right)\left(\frac{I^{334}}{I^{280}}\right) \quad (5)$$

where I^{280} and I^{334} are the lamp intensities of excitation light, ϵ^A and ϵ^D are the molar absorption coefficients of acceptor and donor at the wavelengths indicated, and F^D and F^{DA} are the fluorescence intensities of donor alone and donor in the donor/acceptor pair at acceptor emission maximum using the excitation wavelength indicated.

(*C*) *Time-Resolved Energy-Transfer Measurements.* (*1*) *Donor/Acceptor Decay.* The fluorescence decay $i_D(t)$ of donor (GP-Nap), acceptor (GP-X-Dan), and donor/acceptor (GP-X-DanNap) glycopeptides were analyzed by the sum of exponentials described by

$$I_D(t) = \sum_i^n \alpha_i \exp\left(-\frac{t}{\tau_i}\right) \quad (6)$$

where α_i and τ_i are the amplitude (expressed in percentage) and lifetime of the ith component. The α_i and τ_i values for the donor, or each acceptor with and without donor, were obtained by conventional nonlinear least-squares fit of the emission decay (Grinvald & Steinberg, 1974). The goodness of fits was judged by several criteria: the value of reduced χ^2, randomness of the weighted residuals, and randomness of the autocorrelation of the residuals. The reduced χ^2 is defined by (O'Connor & Phillips, 1984)

$$\chi^2 = \frac{1}{N - P - 1}\sum_{j=1}\frac{[i(t_j) - i^c(t_j)]^2}{i'(t_j)} \quad (7)$$

where $i'(t_j)$ is the measured fluorescence intensity at time t_j, $i(t_j)$ is the measured intensity after background correction, $i^c(t_j)$ is the calculated intensity, N, is the total number of data points (typically 500–1000), and P is the number of fitting parameters. For photon counting data with Poisson noise, a good fit should give χ^2 close to 1.0 (Bevington, 1969). Moreover, we also plot the weighted residuals and autocorrelation of the residuals (Grinvald & Steinberg, 1974) to make sure there are no appreciable correlations among residuals.

(*2*) *Distance Distribution Analysis of Donor Decay.* To analyze the donors' decay as a distribution of populations of donor separation from acceptor several assumptions were made: (1) The multiexponential decay of donor in the absence of acceptor is not due to excited-state reactions on the time scale of the measurement. The two decays observed for the donor are either due to ground-state heterogeneity or are because the excited-state reactions take place so fast that they are already completed when the energy transfer measurement starts. The donor (GP-Nap) has a measurable lifetime that is dominated by one exponential decay of 27 ns (96%). A minor 5.4-ns (4%) component contributes little. Therefore, this assumption is not essential in this case. (2) The critical distances R_{oi} of each of the exponentials are the same, i.e., $R_{oi} = R_o$. Since R_o is almost always determined from the spectral overlap of donor emission with acceptor absorption and the quantum yield of the donor, both of which are already average quantities in the case of multiexponential decays, it's not meaningful to reassign each decay component of the donor a different R_o, though in principle R_o may differ (Haas et al., 1975). It appears that partial determination of R_o for each component decay may be possible, albeit difficult, if the species-associated spectra and lifetimes of each component are determined. In our case, again due to the one dominant component of the donor lifetime, this assumption can be regarded as safe. (3) The orientation between donor and acceptor is random. This assumption is valid since there are several single bonds that link donor and acceptor and in solution single bonds at ends are free to rotate (Haas et al., 1978). (4) The intramolecular diffusion between the donor and acceptor during the lifetime of the donors' excited state can be ignored. The intramolecular diffusion of the ends of flexible polymers have an estimated diffusion constant of $<10^{-7}$ cm^2/s (Haas et al., 1978), corresponding to diffusion of the ends of the molecule of <4 Å during the donors' lifetime (27 ns). In our case the rigidity of the oligosaccharide suggests the actual intramolecular diffusion to be appreciably lower, on the nanosecond time scale.

The donor decay in the presence of acceptor can be written as

$$I_{DA}(t) = \sum_{k=1}^m A_k \int P_k(r)\sum_{i=1}^n \alpha_i e^{-(t/\tau_i)(1 + (R_o/r)^6)}\, dr \quad (8)$$

where $P_k(r)$ is the probability distribution of distances for one population, $\int P_k(r)\, dr = 1$, m = the total number of populations, and A_k is the amplitude or relative concentration of the kth population. The probability distribution of $P_k(r)$ is modeled by either a Gaussian

$$P_k(r) = \frac{1}{\sigma_k\sqrt{2\pi}}\exp\left(-\frac{(r - \bar{r}_k)^2}{2\sigma_k^2}\right) \quad (9)$$

or a Lorentzian

$$P_k(r) = \frac{1}{\sigma_k\pi}\frac{1}{1 + (r - \bar{r}_k/\sigma_k)^2} \quad (10)$$

where $\bar{r}_k$ is the mean distance and σ_k is related to the full width at half-maximum height (FWHM) by = $2.355\sigma_k$ for Gaussian and FWHM = $2\sigma_k$ for Lorentzian. In eq 8, α_i and τ_i of the donor were obtained independently from the donor decay in the absence of acceptor and were fixed in the analysis, whereas the adjustable parameters are A_k, $\bar{r}_k$, and σ_k. The goodness of fits was judged the same way as in the case of donor alone.

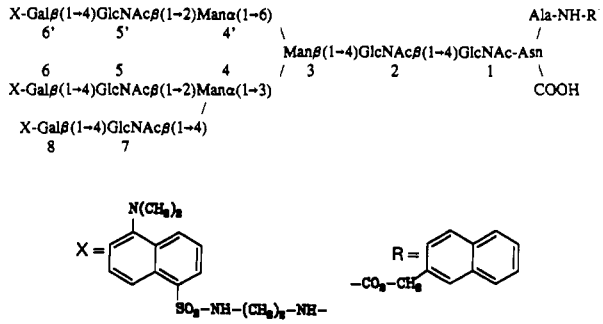

FIGURE 1: Structure of triantennary glycopeptide fluorescence energy-transfer probes. R = naphthyl-2-acetyl. X = dansylethylenediamine, which is attached to the C6 of galactosyl residues located at position 6′, 6, and 8 in the triantennary glycopeptide. GP-Nap contains only R, whereas GP-X-Dan (where X = 6′, 6, or 8) contain only X6′, X6, or X8, and GP-X-DanNap glycopeptides all contain R and either X6′, X6, or X8.

Because the distribution function $P_k(r)$ is unknown, Gaussian (Haas et al., 1975; Lakowicz et al., 1988; Albaugh & Steiner, 1989) or other forms (Haas et al., 1975) were used. Due to the relatively large distribution width of most systems, the ability of decay data to discriminate against alternative forms of distribution is generally minimal. Indeed, we can fit distance distribution of a mutant of Staphylococcal nuclease equally well with either a Gaussian or Lorentzian though the shapes of the two functions are very different (James, Wu, and Brand, unpublished results). However, the decay data in this work do provide preference to Lorentzian form as will be shown under Results.

The integration of distance in eq 8 starts from $0.4R_0$ up to $2.2R_0$ in a 0.1-Å step. This essentially covers all detectable energy-transfer distances. The fits were performed on either a micro-VAX II computer or an HP835 computer. The program was tested by using simulated decay data. All the recovered parameters were within 5% of the known input parameters.

Results

Binding Potency of Glycopeptides to the ASGP-R. Inhibition assays were conducted to establish the relative affinity of GP-X-DanNap (X = 8, 6, and 6′) glycopeptides (Figure 1) compared to unmodified triantennary glycopeptide for binding to the ASGP-R. The resulting I_{50} values determined (the concentration of inhibitor to reduce ^{125}I-ASOR binding by 50%) were 40, 50, 40, and 200 nM for unmodified triantennary, GP-6′-DanNap, GP-8-DanNap, and GP-6-DanNap, respectively. Thereby, only the GP-6-DanNap isomer showed a slight reduction (4-fold) in affinity for the receptor.

Steady-State Energy-Transfer Measurement. The efficiency of energy transfer was determined by steady-state analysis utilizing eq 4. F^D is the integrated area of the donor excitation or emission spectrum (GP-Nap), and F^{DA} is the area of the donor excitation or emission spectra (Figure 2) of equimolar samples containing both the donor and acceptor (GP-6-DanNap, GP-6′-DanNap, and GP-8-DanNap). Equimolarity of the glycopeptides was confirmed by quantitative monosaccharide analysis of glucosamine after hydrolysis with hydrochloric acid (Hardy et al., 1988). The measured energy-transfer efficiencies illustrate that in each isomer the donor is quenched to a different extent. This translates to a measured average distance $\langle r \rangle$ of 18.6, 21.3, and 20.4 Å for the GP-6′-DanNap, GP-6-DanNap, and GP-8-DanNap isomers, respectively (Table I).

Steady-State Energy Transfer Using RP-HPLC. Steady-state energy-transfer efficiency was also measured by use of

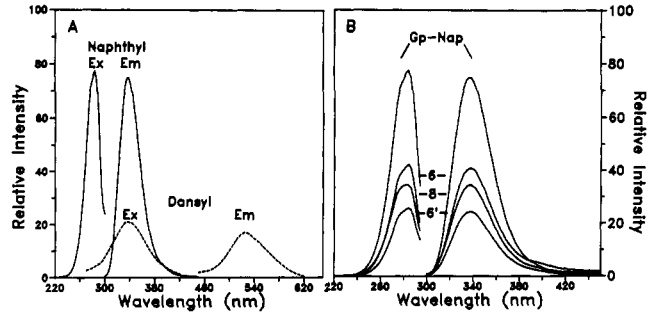

FIGURE 2: Fluorescence spectra of labeled glycopeptides. (A) The uncorrected excitation and emission of spectra of GP-Nap (naphthyl, —) and GP-8-Dan (dansyl, - - -), illustrating the overlap of naphthyl-2-acetyl emission with dansyl excitation spectra. The samples are compared at equimolarity illustrating a 4-fold higher intensity for the naphthyl-2-acetyl fluorophore. (B) Comparison of uncorrected excitation and emission spectra of GP-Nap and GP-X-DanNap (X is either 6, 8, or 6′) glycopeptides compared at equimolarity. The reduced intensities of GP-X-DanNap spectra are due to differential intramolecular quenching of the naphthyl-2-acetyl.

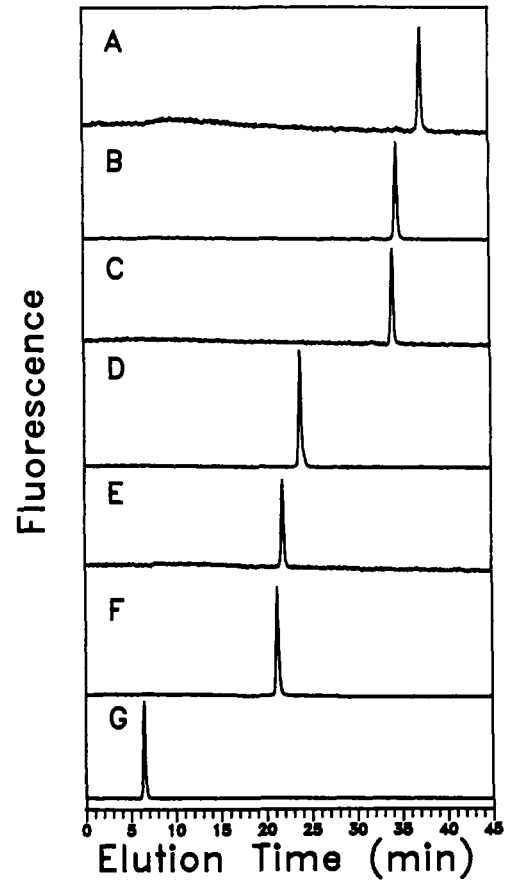

FIGURE 3: RP-HPLC chromatography of individual fluorescent glycopeptides. Each donor/acceptor glycopeptide, (A) GP-6′-DanNap, (B) GP-8-DanNap, and (C) GP-6-DanNap, acceptor-only glycopeptide, (D) GP-6′-Dan, (E) GP-6-Dan, and (F) GP-8-Dan, and donor-only glycopeptide (G) GP-Nap, was chromatographed on octyl RP-HPLC eluted as described under Materials and Methods, detecting the eluting glycopeptides by fluorescence.

the integrated peak area of glycopeptides eluting from RP-HPLC detected at selective excitation and emission wavelengths. Each glycopeptide was injected onto RP-HPLC, eluted under gradient, and detected by the fluorescent chromophore (Figure 3). With a prepared mixture of all seven glycopeptides, four consecutive injections were performed, with only the wavelength and mode of detection changing (Figure 4A–D). The integration area of each peak was determined

Table I: Average Efficiency $\langle E \rangle$ and Distance $\langle r \rangle$ Separating Donor and Acceptor in Glycopeptides

	GP-6′-DanNap		GP-6-DanNap		GP-8-DanNap	
	$\langle E \rangle$ (%)	$\langle r \rangle$ (Å)	$\langle E \rangle$ (%)	$\langle r \rangle$ (Å)	$\langle E \rangle$ (%)	$\langle r \rangle$ (Å)
donor quenching[a]	66	18.6	46	21.3	53	20.4
RP-HPLC donor quenching[b]	74	17.4	43	21.8	68	18.3
RP-HPLC sensitized emission[c]	70	17.0	43	21.8	69	18.4
average lifetime[d]	75	17.3	57	19.9	62	19.5

[a] Steady-state analysis by integration of excitation or emission band. [b] Naphthyl-2-acetyl quenching as measured by integration area of Figure 4B. [c] Dansyl sensitized emission as measure by integration area of Figure 4C,D. [d] Data determined using $\langle \tau \rangle$ (Table II).

with use of Spectra Physics Chromjet integrator, and the error in analysis was measured to be 1% by performing repeated sample injections.

The sample containing all seven glycopeptides was chromatographed on RP-HPLC, and the absorbance at 220 nm was monitored (Figure 4A). This data allowed for the normalization of peak area for GP-Nap and GP-X-DanNap (X = 6, 8, and 6′) samples, accounting for the percent overlap of the dansyl absorption chromophore by comparison to GP-X-Dan integration areas. A second application of the sample allowed monitoring of the naphthyl-2-actyl group preferentially by fluorescence detection with excitation at 280 nm and emission at 340 nm (Figure 4B). The ratio of peak area for GP-X-DanNap glycopeptides was lower relative to GP-Nap as compared to the same peaks in panel A. The loss of emission intensity for GP-X-DanNap glycopeptides is attributable to intramolecular quenching of the donor. Differential quenching between the three GP-X-DanNap glycopeptides was observed, indicating differences in efficiencies of energy transfer for the three isomeric glycopeptides. The peak areas determined for each energy-transfer sample and GP-Nap, after normalization of concentrations, were used as input data in eq 4 to calculate the average efficiency. The determined efficiencies allowed calculation of the average distance $\langle r \rangle$ separating the donor and acceptor by eq 3.

An alternative efficiency measurement, termed sensitized emission of acceptor, was performed on RP-HPLC by detecting the eluting glycopeptides with two excitation wavelengths of 280 and 334 nm and a single emission of 520 nm. The direct excitation of dansyl at 334 nm allowed the detection of GP-X-Dan and GP-X-DanNap peaks but not of GP-Nap (Figure 4C). The integrated peak areas from panel C were used to normalize relative molar concentrations of the glycopeptides and in conjunction with data from panel D were used for the calculation of efficiency by sensitized emission of the acceptor (Stryer, 1978). Chromatography of the glycopeptides with fluorescence detection using an excitation of 280 nm and emission of 520 nm produced the chromatogram illustrated in Figure 4D. The increase in peak areas for GP-X-DanNap peaks relative to GP-X-Dan peaks in Figure 4D as compared to the relative ratio of the same peaks in Figure 4C is due to sensitized emission of the acceptor on samples containing donor. The peak areas from Figure 4C,D, the relative molar absorptivity of dansyl and naphthyl-2-acetyl at 280 and 334 nm determined from absorbance spectra of glycopeptides, and the relative lamp intensity (I) at the two excitation wavelengths were used to calculate the efficiency of energy transfer using eq 5. The calculated efficiencies, for GP-X-DanNap glycopeptides, detrmined by sensitized emission as well as the average distances $\langle r \rangle$ calculated from these efficiencies using eq 3, are included in Table I.

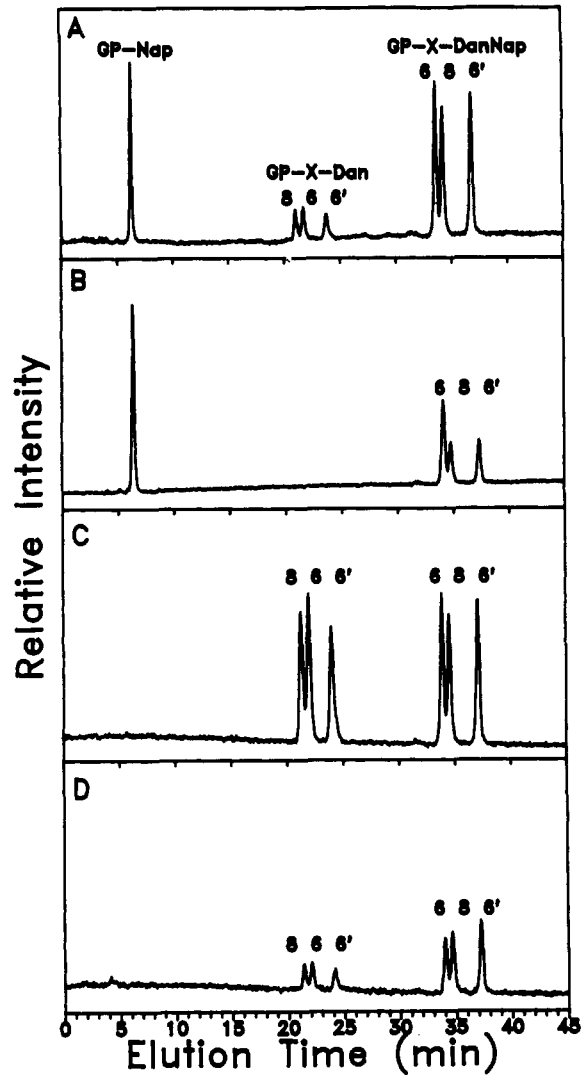

FIGURE 4: Efficiency of energy-transfer measurement on RP-HPLC. A prepared mixture of GP-Nap, GP-X-Dan, and GP-X-DanNap glycopeptides (X is either 6, 8, or 6′) was subjected to RP-HPLC separation using the conditions described under Materials and Methods. The detection was (A) UV at 220 nm 0.05 AUFS (base-line corrected), (B) fluorescence with ex = 280 nm and em = 340 nm, (C) fluorescence with ex = 334 nm and em = 520 nm, and (D) fluorescence ex = 280 nm and em = 520 nm.

Multiexponential Analysis of Time-Resolved Fluorescence Decay Data. The acceptor decay (excited at 340 nm where naphthyl-2-acetyl has no absorption) were analyzed by three exponentials (Table II). The average decay of the acceptor (dansyl) on the glycopeptide is not influenced by attachment of the donor (naphthyl-2-acetyl) group. Thus, there is no direct contact between the two fluorophores in the derivitized glycopeptide.

The naphthyl-2-acetyl group in GP-Nap glycopeptide can be analyzed by two exponentials with one major component having a lifetime (τ) of 27 ns and a minor component having a lifetime (τ) of about 5–6 ns as shown in Table II. This minor component was always there when the donor decays of different preparations were measured. Thus, we think this component is not due to an impurity.

The donor decay of the glycopeptides (GP-X-DanNap) was analyzed similarly by multiexponentials. This type of empirical analysis is useful to obtain some average properties of the system. For energy transfer experiments here, the results also qualitatively indicate whether there is a distance distribution or not.

Table II: Nonlinear Least-Squares Fit of Donor or Acceptor Lifetime

	dansyl[b]			naphthyl-2-acetyl[b]		
sample	α_i	τ_i	$\langle\tau\rangle^c$	α_i	τ_i	$\langle\tau\rangle^c$
GP-Nap				0.954	27.00	
				0.046	5.41	26.00
GP-8-DanNap	0.299	4.04		0.089	21.16	
	0.422	2.40	2.30	0.814	9.75	
	0.279	0.30		0.097	1.95	10.01
GP-6-DanNap	0.220	4.84		0.542	17.32	
	0.543	2.80	2.67	0.189	7.37	
	0.237	0.41		0.269	0.77	10.99
GP-6′-DanNap	0.093	5.99		0.075	17.52	
	0.686	3.08	2.85	0.592	8.02	
	0.221	0.85		0.333	1.16	6.45
GP-8-Dan	0.328	3.80				
	0.394	2.11	2.15			
	0.278	0.27				
GP-6-Dan	0.288	4.38				
	0.458	2.57	2.54			
	0.254	0.42				
GP-6′-Dan	0.176	4.72				
	0.558	2.50	2.33			
	0.266	0.41				

[a] The amplitude (α) and lifetime (τ) in nanoseconds were determined by nonlinear least-squares fits of the dansyl decay when exciting at 340 nm and monitored by emission at 520 nm. [b] The amplitude (α) and lifetime (τ) in nanoseconds were determined by nonlinear least-squares fits of the naphthyl-2-acetyl decay when exciting at 290 nm and monitoring emission at 350 nm. [c] The average lifetime $\langle\tau\rangle = \sum\alpha_i\tau_i$.

Three exponentials were required to fit the donor decay in the donor/acceptor pairs as shown in Table II. Compared to the decay of donor alone, the fluorescence decay of naphthyl-2-acetyl in GP-X-DanNap is very heterogeneous, indicating the existence of distance population(s) between the donor and acceptor. We can use another criterion to show that there is a distance distribution. Defining the amplitude-weighted lifetime as $\langle\tau\rangle_A = \sum\alpha_i\tau_i$, and the intensity-weighted lifetime as $\langle\tau\rangle_I = \sum\alpha_i\tau_i^2/\sum\alpha_i\tau_i$, then the ratio $A = \langle\tau_{DA}\rangle_A/\langle\tau_D\rangle_A$ should be equal to the ratio $B = \langle\tau_{DA}\rangle_I/\langle\tau_D\rangle_I$, if there is no distribution (Albaugh et al., 1989). A value of B/A > 1 indicates there is a distance distribution. Indeed, using the data in Table II, we get B/A = 1.12, 1.42, 1.43 for the isomers with acceptor attached to either Gal 8, 6, or 6′, respectively. Thus, distribution analysis is required to describe the data adequately. It is pertinent to note that the amplitudes and lifetimes of each isomer are different. These may indicate that different isomers have different distance distribution(s).

To obtain the average energy-transfer efficiencies from the lifetime measurements (Table I), the average lifetime (Table II) of the donor glycopeptides $\langle\tau_D\rangle$ and donor/acceptor glycopeptides $\langle\tau_{DA}\rangle$ were substituted for the F_D and F_{DA} in eq 4. The average distance $\langle r\rangle$ values calculated from lifetime measurements using eq 3 are presented in Table I.

Distance Distribution Analysis. As discussed above, a distribution of distances is necessary to fit the decay data. We used eq 8 to obtain the distance distribution(s) of the glycopeptides. Parts A and B of Figure 5 show the fits to the decay data of GP-8-DanNap using a Gaussian (5A) and a Lorentzian distance distribution. The fit to a Gaussian is clearly not good as judged from the residuals and the corresponding autocorrelation. In contrast, a Lorentzian fit appears to be satisfactory. In the following, we will use Lorentzian distributions to analyze the decay data of the glycopeptides.

The average distance separating the fluorophores of GP-8-DanNap is about 19 Å while the FWHM is surprisingly small, only about 1.5 Å. Numerical experiments were done

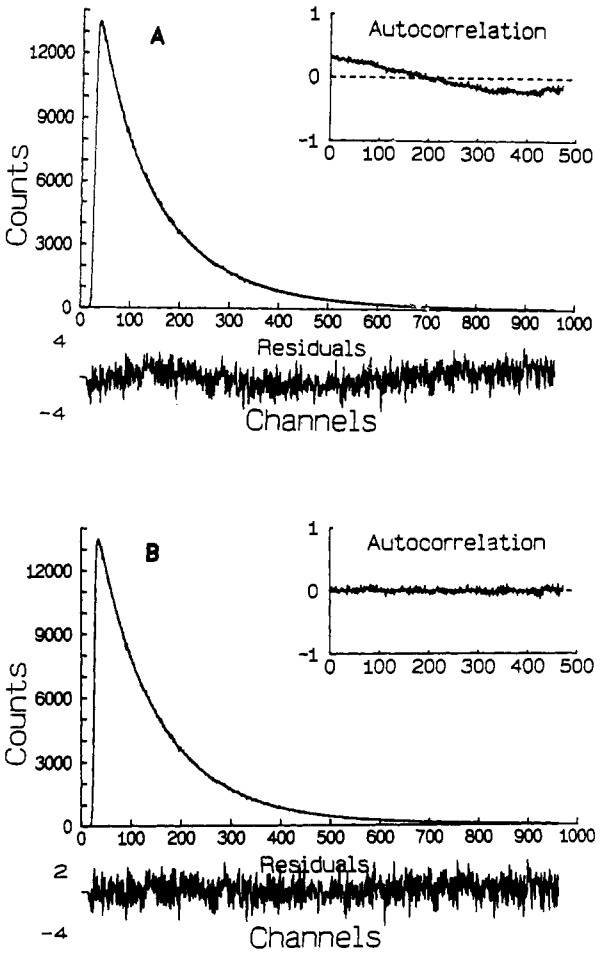

FIGURE 5: Distance distribution fits to decay data of GP-8-DanNap at excitation 290 nm and emission 350 nm. (A) Measured and fitted decay curves (almost identical) vs channel number (0.088 ns/channel). The weighted residuals are plotted at the lower part. (Inset) Autocorrelation of the residuals. The fitting function is a Gaussian (eq 9). (B) Measured and fitted decay curves vs channel number for a Lorentzian fit (eq 10). Weighted residuals and autocorrelations of the fit are also shown.

to evaluate the sensitivity of the data to the width of the distribution. The average distance was allowed to be a free-running parameter in the analysis for a series of fixed values of FWHM and the optimized average distance changed by less than 1 Å for a fixed FWHM from 0.8 to 1.8 Å. Parts A–D of Figure 6 show the autocorrelation functions of the residuals obtained for each of the fits. Even an attempted fit at a FWHM fixed only 0.5 Å away from the optimum value causes a significant deviation from linearity in the autocorrelation of the residuals. Figure 6E shows the changes in χ^2 as the distribution is varied systematically.

While the fluorescence decay data of GP-8-DanNap can be adequately fit by one Lorentzian distance distribution, those of GP-6-DanNap and GP-6′-DanNap require two Lorentzian distributions with a totally different average distance for each distribution. Figure 7A shows a one-Lorentzian fit, and Figure 7B shows a two-Lorentzian fit to the decay data of GP-6-DanNap. The average distances of the two populations are about 22 and 10 Å. We have tried to fit the decay with one Gaussian or Lorentzian distribution modified by an asymmetric factor (Wiczk et al., 1990) (left half not equal to right half) and were unable to get a good fit. Thus, a two-population fit is necessary, which is also true for GP-6′-DanNap. Experiments were performed with two separately prepared samples of GP-6-DanNap and GP-6′-DanNap isomers. In all

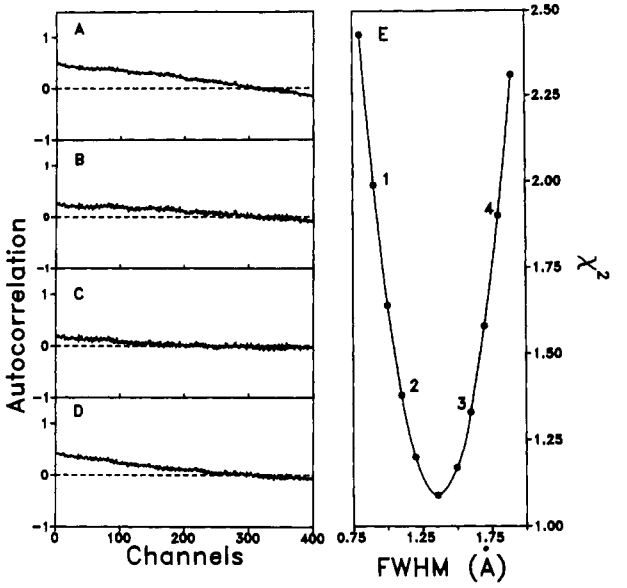

FIGURE 6: Sensitivity analysis of the fits to decay data of GP-8-DanNap. Panels (A–D): autocorrelation functions of the optimized fits with FWHM fixed at 0.80 Å (A), 1.10 Å (B), 1.60 Å (C), and 1.80 Å (D). Panel E shows the χ^2 values at different fixed FWHM values. The data set is the same as in Figure 5. For comparison refer to the autocorrelations of the best fit in the inset of Figure 5B.

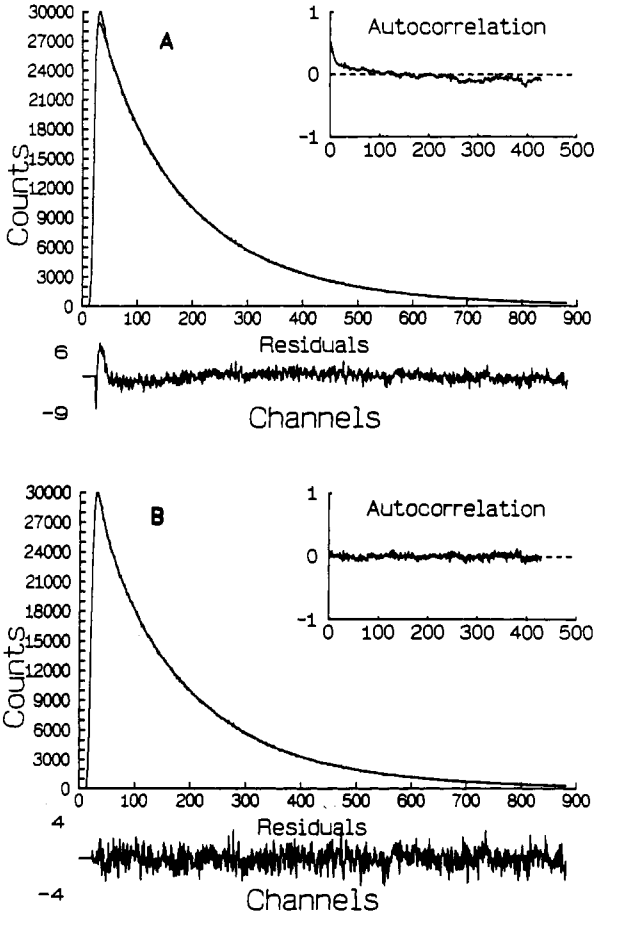

FIGURE 7: Lorentzian fit to the decay data of GP-6-DanNap. Conditions are the same as in Figure 5. (A) One-Lorentzian fit. (B) Two-Lorentzian fit.

experiments a two-population model gave the best fit to the data for these two isomers. The relative concentration of each population is emission wavelength independent from 330 to 370 nm, suggesting that the second population is not due to an impurity component. We also measured the decay of GP-6-DanNap with a microchannel plate PMT with a full width at half-maximum of about 80 ps (compare to about 550 ps for conventional PMT used in this work) and got very similar results (not shown). Thus, the two-population fit for GP-6-DanNap and GP-6′-DanNap is not due to experimental artifacts.

Table III: Population Distribution of Donor/Acceptor Distance

sample[a]	A_i (%)[b]	⟨r⟩ (Å)[b]	FWHM (Å)[c]
GP5-8-DanNap	1.0	19.02 ± 0.01	1.59 ± 0.04
GP5-6′-DanNap	0.60 ± 0.01	18.29 ± 0.01	0.58 ± 0.02
	0.40 ± 0.01	11.71 ± 0.07	2.90 ± 0.49
GP5-6-DanNap	0.62 ± 0.01	21.70 ± 0.02	1.70 ± 0.45
	0.38 ± 0.01	9.70 ± 0.20	2.90 ± 0.64

[a] All data represent the average and standard deviation of three determinations. [b] The resulting amplitudes (A_i) and average distance values ⟨r⟩ were determined by fitting the naphthyl-2-acetyl decay curve for energy-transfer glycopeptides to a Lorentzian function (eq 10). [c] The full width at half-maximum height of each population of donor/acceptor pair.

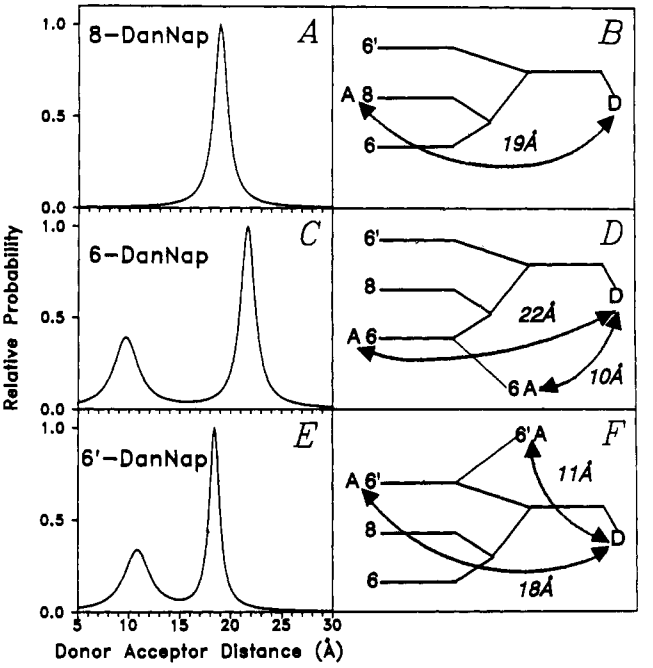

FIGURE 8: Donor/acceptor population distributions. Lorentzian fit of the donor decay curves and illustrated results for GP-8-DanNap (A, B), GP-6-DanNap (C, D), and GP-6′-DanNap (E, F). The plots (left) indicate the probability of a donor/acceptor population occurring at different distances in the triantennary glycopeptide. The ratio of populations for GP-6-DanNap and GP-6′-DanNap were determined to be approximately 60% of the extended conformation and 40% of the folded form. The illustrations (right) show a single double-headed arrow of defined length for each donor (D) to acceptor (A) distance determined.

The results of Lorentzian fits to the three glycopeptides are shown in Table III and are plotted in Figure 8. The GP-8-DanNap glycopeptide had a singly distributed population of donor/acceptor with an average separation distance of 19 Å and a narrow width of 1.59 Å at half-height (Figure 8A). This result is illustrated pictorially in Figure 8B by a single double-headed arrow of defined distance separating the donor (D) from acceptor (A) in GP-8-DanNap. The GP-6-DanNap glycopeptide contained two populations of donor/acceptor distances, one with a longer separation distance of 21.7 Å and narrow width at half-height of 1.7 Å and a second shorter separation distance of 9.7 Å with broader width at half-height of 2.9 Å (Figure 8C). Likewise, the Lorentzian fit for the

decay data of the GP-6′-DanNap glycopeptide also revealed two populations of donor/acceptor distances. The major population has an average separation distance of 18.3 Å with width of 0.58 Å at half-height (Figure 8E), and the minor population exhibited a shorter separation distance that was centered around 11.7 Å and also showed a broader distribution of 2.9 Å at half height. These data are represented in parts D and F of Figure 8 illustrated by two double-headed arrows of different lengths corresponding to the two populations for each isomer. The short distances arise from the semiflexibility of the indicated branch showing it folds back allowing the acceptor to make a close approach to the donor.

Discussion

Application of Steady-State Energy-Transfer Measurements To Study Complex Carbohydrates. Our approach to studying the solution conformation of the triantennary glycopeptide is to apply the techniques of steady-state and time-resolved fluorescence energy transfer to determine the distances between a permanently fixed donor located at the N terminus of the glycopeptide and an acceptor attached to the terminal Gal residue of one of each antenna of the oligosaccharide. The steady-state analysis indicates that dansyl and naphthyl-2-acetyl derivatives are well suited for energy-transfer studies on complex oligosaccharides. The derived Förster distance, R_0, (the distance of 50% energy-transfer efficiency) was 20.8 Å, which is in close agreement with the R_0 reported by Haas et al. (1975) (22 Å) for the same donor and acceptor determined in glycerol solution. The average distance determined for each branch isomer of the triantennary glycopeptide was close to the R_0 distance, allowing for maximum sensitivity for measuring small changes in donor/acceptor distance. Although dansyl and naphthyl-2-acetyl groups provided a suitable R_0 for the distances spanned in this study, selection of fluorophores with a different R_0 value would allow energy-transfer measurements up to 100 Å, which might find utility on larger polylactosamine-containing complex oligosaccharides.

The inherent high sensitivity of fluorescence energy-transfer measurements makes possible conformational studies on complex oligosaccharides utilizing 2 orders of magnitude less sample than required for multidimensional NMR measurements. The use of RP-HPLC with fluorescence detection to simultaneously separate and detect fluorescent glycopeptide probes containing donor, acceptor, and donor/acceptor provides a means of conducting microscale steady-state energy-transfer measurements. In this application picomole quantities of sample were used to determine efficiency of energy transfer on chromatographically resolved oligosaccharides. Minor changes in eluant concentration due to gradient elution had negligible effect of quenching the fluorophores or changing the quantum yield of the donor or acceptor as evidenced by the relative agreement of the data with that derived from steady-state scanning fluorescence. When used in this way, energy transfer may extend presently existing oligosaccharide HPLC mapping techniques (Tomiya et al., 1987) to provide oligosaccharide conformation as well as primary structure.

Distance Distributions by Time-Resolved Energy-Transfer Measurements. In addition to the average distance, time-resolved energy-transfer measurements may be used to reveal the distribution of populations of donor/acceptor distances. This application was demonstrated in a previous study (Haas et al., 1975), where the same fluorophores were attached to a series of completely flexible peptides and the donor lifetime measurements were fit to Gaussian distributions of distances separating the donor from the acceptor. The longest distance measured contained the donor spaced by nine L-glutamine residues from the acceptor and had a average separation distance of 21 Å. The distribution of distances measured for this probe was a single population that spanned from 7 to 35 Å, indicating a broad end–end distribution for completely flexible polypeptides.

In contrast, the antenna of complex oligosaccharides are considered to be semirigid polymers, and thus the donor/acceptor distance may be expected to have more narrowly defined populations. Also, lifetime measurements conducted on the nanosecond time scale occur faster than intramolecular diffusion of the flexible branches, which can lead to a quantitative determination of more than one population of donor/acceptor distance. These aspects of time-resolved energy-transfer measurements are illustrated by comparison of the Lorentzian fit of the data for the three isomeric glycopeptide probes. The distribution determined from the lifetime data for GP-8-DanNap shows a single population that only spans 1.5 Å in width at half-height. The GP-6-DanNap and GP-6′-DanNap glycopeptides both showed two populations of donor/acceptor distances.

For GP-6′-DanNap this might be anticipated since the Manα(1→6)Man linkages in other oligosaccharides are flexible as determined from NMR data (Homans et al., 1986, 1987a; Brisson & Carver, 1983a). The flexibility of this glycosidic linkage apparently leads to conformational heterogeneity, allowing the detection of a population in an extended conformation (18 Å) an a second population that is folded (about 12 Å). However, this linkage might not be the only contribution to the observed two populations as will be discussed below.

Similarly, GP-6-DanNap shows two populations, indicating that there is at least one linkage between Gal 6 and GlcNAc 1 that is capable of adopting two somewhat rigid conformations so that one population is extended (22 Å) and the other is folded (<10 Å). Since both GP-8-DanNap and GP-6-DanNap contain acceptors attached to the core through the same Manα(1→3)Man linkage, this linkage and other common glycosidic linkages cannot be considered as the site of flexibility. These two isomers differ in their linkage of Galβ(1→4)GlcNAc to Manα(1→3)Man (GP-6-DanNap is β(1→2) whereas GP-8-DanNap is β(1→4)), producing a different relative spatial orientation of the two branches with respect to the third branch. The GlcNAcβ(1→2)Man can adopt folded-back structures (Brisson & Carver, 1983c) deduced from the NMR data while other conformations cannot be excluded within the uncertainties of those measurements. Also, it has been shown that the conformation of this linkage depends on other glycosidic conformations in the molecule (Cumming & Carver, 1987a). Moreover, the conformation of an isolated disaccharide may not necessarily be the same as that of the identical disaccharide inserted in an oligosaccharide chain since there may be more interactions that determine the overall conformation of the chain. Thus, we observe a previously unidentified flexible branch in the GP-6-DanNap glycopeptide that we speculate arises from flexibility about the GlcNAcβ-(1→2)Man linkage in the intact oligosaccharide.

We discuss here the reliability of the structural parameters obtained from time-resolved fluorescence energy-transfer measurements. As mentioned under Data Analysis, we used several assumptions in analyzing our decay data of energy transfer. These might affect some of the results were they rigorously incorporated. In the following, we focus on several aspects of the results. The number of populations of distances or whether the distance distribution is unimodal or multimodal

in shape is well-defined regardless of the assumptions used. The fluorescence energy-transfer rate is proportional to the inverse of the sixth power of distance so that the rate changes drastically as distance varies (cf. eq 8). Since the decay of donor alone is nearly a single exponential, the shape of the distance distribution is apparent by direct inspection of the decay data of donor in the donor/acceptor pair (Table II). If a distance distribution is unimodal, then an empirical multiexponential analysis of donor decay in the donor/acceptor pair should produce several apparent lifetimes that mimic the shape of the distribution. For GP-8-DanNap, this is the case as the amplitudes of the shorter and longer lifetime components are symmetrically distributed around that of the center lifetime (Table II). For Gp-6′-DanNap and GP-6-DanNap, the distribution is clearly not unimodal since the amplitude of the shorter lifetime is not approximately equal to that of the longer component. As shown in the Results section, this asymmetry cannot be approximated by a smooth unimodal asymmetric distribution. A bimodal distribution has to be used. As in any other data analysis, these are the minimal number of parameters to approximate the experimental data.

The use of a Lorentzian function (eq 10) is only an approximation to the actual distance distribution. Theoretical modeling of polymers leads to a closed expression of distance distribution only when the polymer is completely flexible. For a randomly coiled peptide in solution many average properties have been calculated numerically (Flory, 1969) where a distribution is implicitly used. For semirigid molecules such as double-strand DNA or polysaccharides with finite elasticity, it is more difficult to obtain an expression of the distance distribution that can be handled easily in data analysis. Therefore, parameterized models such as Gaussian and Lorentzian functions are one way to analyze data to obtain meaningful results. In the course of analyzing real and simulated data, we found that the average distance of a distribution can be determined quite precisely while the shape of the distribution is determined with less accuracy. For example, in the case of GP-8-DanNap, we have shown in the Results section (parts A and B of Figure 5) that a single Gaussian distance distribution did not fit the measured data while a single Lorentzian fit was quite satisfactory. However, we could also get equally good fit with two Gaussian distance distributions for the same data. If we superimpose the two Gaussians, we then get one population back. The average distance of the two superimposed Gaussians is the same as that of a Lorentzian. The shape of the superposition on the other hand is slightly different from that of a Lorentzian. It is likely that some degrees of compensation can occur for the probability of distances near the average population when different model functions are used. This does not alter our conclusions about the populations of the glycopeptides, but it does point out the danger of overinterpreting the exact shape of the distance distributions here. Note that we are comparing here the results of fitting two different model functions to the experimental data. This is different from the robustness of fit to the Lorentzian function, which was quite good as we have shown in the Results section.

The average distances of the two populations for GP-6-DanNap and GP-6′-DanNap are quite different. A question that may arise is whether there is a continuous distribution of distances between the two populations if flexibility exists in the GlcNAcβ(1→2)Man linkage or in Manα(1→6)Man linkage. This is an unlikely possibility because in energy-transfer measurements the strong distance dependence of rate will detect these intermediates in the data analysis if the population is substantial. Furthermore, our work in progress on the temperature dependence of energy transfer shows that there is a potential barrier between the two populations for each isomer. Consequently, the conformers with intermediate distances are unlikely to populate to an appreciable level. It is reasonable to propose that for the GP-6-DanNap and GP-6′-DanNap isomers, there are two populations that are clustered in the vicinity of their average distances and the two populations interconvert slowly, allowing their detection on the time scale of the energy transfer measurement.

Biological Relevance of the Solution Conformation of the Triantennary Glycopeptide. Fluorescent energy-transfer measurements on oligosaccharides may reveal distances that deviate from those derived from theoretical calculation or from NMR solution measurements. These deviations may be due to true conformational populations that are not detectable by other approaches or may be due to artificial populations that arise after attachment of the fluorescent probe to a given branch. We have tried to address the later concern by examining the binding affinity of the derivitized oligosaccharides to a naturally occurring receptor. Comparison of these data shows that attachment of the dansyl group to Gal 6 sacrifices binding affinity to the receptor by 4-fold. This is a result identical with that previously reported when a photoaffinity probe is attached to Gal 6 (Rice et al. 1990) and appears to be due to some degree of steric hindrance at the binding site for Gal 6. However, the observation that the remaining fluorescent probes bind with equivalent affinity as the unmodified triantennary suggests that these modified glycopeptides exist in the same solution conformation as the unmodified glycopeptide or are capable of achieving a biologically correct conformation in order to bind with high affinity to the ASGP-R.

Previously we reported that a photoaffinity label attached to either Gal 6 or 6′ of the triantennary glycopeptide each specifically labeled the major subunit (RHL1) of the ASGP-R of rat hepatocytes, whereas photoaffinity labeling with the reagent attached to Gal 8 only labeled the minor subunits (RHL2/3) of the receptor, indicating a nonrandom binding geometry between the ligand and the lectin (Rice et al., 1990). These data, in light of the present study, suggest that the unique rigidity detected for the antennae in GP-8-DanNap may allow the RHL2/3 subunits of the ASGP-R to identify it. Coincidentally, both flexible antennae position Gal 6 and 6′ for proper binding to the ASGP-R such that they are only recognized by the RHL1 subunit. Perhaps these observations are suggestive to conformational changes in the triantennary glycopeptide ligand on binding to the ASGP-R that result in its observed high specificity and affinity.

Although the present study was limited to the examination of a single type of triantennary structure, fluorescence energy transfer could be utilized to study a wide array of complex glycopeptides and oligosaccharide structures and substructures to determine distances and solution conformation. An understanding of complex oligosaccharide conformation and dynamics may lead to an improved understanding of physiological functions of this class of biopolymers.

Registry No. Ala-Asn glycopeptide, 133984-15-3.

References

Albaugh, S., & Steiner, R. F. (1989) *J. Phys. Chem. 93*, 8013–8016.

Albaugh, S., Lan, J., & Steiner, R. F. (1989) *Biophys. Chem. 33*, 71–76.

Badea, M., & Brand, L. (1979) *Methods Enzymol. 61*, 378–425.
Bevington, P. R. (1969) *Data Reduction and Error Analysis for the Physical Sciences*, McGraw-Hill Book Company, New York.
Bock, K., Arnarp, J., & Lönngren, (1982) *Eur. J. Biochem. 129*, 171–178.
Brisson, J. B., & Carver, J. P. (1983a) *Biochemistry 22*, 1362–1368.
Brisson, J. B., & Carver, J. P. (1983b) *Biochemistry 22*, 3671–3680.
Brisson, J. B., & Carver, J. P. (1983c) *Biochemistry 22*, 3680–3686.
Cummings, D. A., & Carver, J. P. (1987a) *Biochemistry 26*, 6664–6676.
Cummings, D. A., & Carver, J. P. (1987b) *Biochemistry 26*, 6676–6683.
Cummings, D. A., Shah, J. J., Krepinsky, A. A., Grey, A. A., & Carver, J. P. (1987) *Biochemistry 26*, 6655–6663.
Eaton, D. (1988) *Pure Appl. Chem. 60*, 1107–1114.
Edge, C. J., Singh, U. C., Bazzo, R., Taylor, G. L., Dwek, R. A., & Rademacher, T. W., (1990) *Biochemistry 29*, 1971–1974.
Englert, A., & Leclerc, M. (1978) *Proc. Natl. Acad. Sci. U.S.A. 75*, 1050–1051.
Fairclough, R., & Cantor, C. R. (1977) *Methods Enzymol. 48*, 347–379.
Flory, P. J. (1969) *Statistical Mechanics of Chain Molecules*, John Wiley & Sons, New York.
Förster, T. (1948) *Ann. Phys. (Leipzig) 2*, 55–75.
Grinvald, A., & Steinberg, T. Z. (1974) *Anal. Biochem. 59*, 583–598.
Haas, E., Wichek, M., Katchalski-Katzir, E., & Steinberg, I. Z., (1975) *Proc. Natl. Acad. Sci. U.S.A. 72*, 1807–1811.
Haas, E., Katchalski-Katzir, E., & Steinberg, I. Z., (1978) *Biopolymers 17*, 11–31.
Hardy, M. R., Townsend, R. R., & Lee, Y. C., (1988) *Anal. Biochem. 157*, 179–185.
Homans, S. W., Dwek, R. A., Boyd, J., Mahmoudian, M., Richards, W. G., & Rademacher, T. W. (1986), *Biochemistry 25*, 6342–6350.
Homans, S. W., Dwek, R. A., & Rademacher, T. W. (1987a) *Biochemistry 26*, 6553–6560.
Homans, S. W., Pastore, A., Dwek, R. A., & Rademacher, T. W., (1987b) *Biochemistry 26*, 6649–6655.
Homans, S. W., Dwek, R. A., & Rademacher, T. W. (1987c) *Biochemistry 26*, 6571–6578.
Kornfeld, R., & Kornfeld, S., (1985) *Annu. Rev. Biochem. 54*, 631–664.
Lakowicz, T. R., Gryczynski, I., Cheung, H. C., Wang, C. K., Johnson, M. L., & Josh, N. (1988) *Biochemistry 27*, 9149–9160.
Lee, Y. C., Townsend, R. R., Hardy, M. R., Lönngren, J., Arnarp, J., Haraldsson, M., & Lönn, H. (1983) *J. Biol. Chem. 258*, 199–202.
Montreuil, J. (1984) *Pure Appl. Chem. 56*, 859–877.
O'Connor, D. V., & Phillips, D. (1984) *Time-Correlated Single-Photon Counting*, Academic Press, New York.
Rice, K. G., & Lee, Y. C. (1990) *J. Biol. Chem. 265*, 18423–18428.
Rice, K. G., Weisz, O. A., Barthel, T., Lee, R. T., & Lee, Y. C. (1990) *J. Biol. Chem. 265*, 18429–18434.
Stryer, L. (1978) *Annu. Rev. Biochem. 47*, 819–846.
Stryer, L., & Haugland, R. P. (1967) *Proc. Natl. Acad. Sci. U.S.A. 58*, 719–726.
Seglen, P. O. (1976) *Methods Cell Biol. 13*, 29–83.
Tomiya, N., Kurono, M., Ishihara, H., Tejima, S., Endo, S., Arata, Y., & Takahashi, N. (1987) *Anal. Biochem. 163*, 489–499.
Wiczk, W., Eis, P. S., Fishman, M. N., Johnson, M. L., & Lackowicz, T. R. (1990) *Proc. SPIE 1204*, 645–655.